University of Cambridge

Department of Chemical Engineering and Biotechnology

CEBT IB Project 4: Part 1

Design of a Shell and Tube Heat Exchanger

Author: Lev Gerasimov
College: Downing

Executive Summary

This report presents the design of a shell-and-tube heat exchanger for the pasteurisation of orange juice from 25 °C to 98 °C using pressurised hot water at 130 °C. The final configuration selected was a horizontal TEMA BEM exchanger with 66 straight tubes in 6 passes, a square layout, and single-segmental vertical-cut baffles. The design was developed from an initial Kern-method sizing and then refined using Bell's method following Sinnott in order to represent shell-side leakage, bypass, and window effects more realistically. The final geometry was chosen as a balanced compromise between thermal area margin and shell-side pressure drop. The exchanger achieved a Bell-based overall heat-transfer coefficient of $929.6\,\mathrm{W\,m^{-2}\,K^{-1}}$, a required area of $29.33\,\mathrm{m^2}$, and an available area of $31.10\,\mathrm{m^2}$, giving an area margin of 6.0 %. The final pressure drops were 0.276 bar on the tube side and 0.197 bar on the shell side, both below the design limit of 0.5 bar. The selected design therefore satisfies the main thermal and hydraulic requirements while remaining close to standard Sinnott design guidance for tube pitch, baffle cut, and baffle spacing.

Table 1: Executive design summary

Item	Value	Unit / note
Juice temperature	$25 \rightarrow 98$	°C
Water temperature	$130 \rightarrow 110$	°C
Heat duty	1.331	MW
Corrected LMTD	48.83	K
Overall HTC, U	929.6	$\mathrm{W/(m^2\,K)}$
Required area	29.33	$\mathrm{m^2}$
Available area	31.10	$\mathrm{m^2}$
Tube-side pressure drop	0.276	bar
Shell-side pressure drop	0.197	bar
Number of tubes / passes	66 / 6	–
Tube size (OD / ID)	25.0 / 21.8	mm
Tube length	6.0	m

1 Introduction

The aim of this project is to design a **shell-and-tube heat exchanger** for the pasteurisation of orange juice. According to the project brief, the exchanger must heat orange juice from 25 °C to 98 °C using **pressurised hot water** as the heating medium [1]. The design must satisfy both thermal and hydraulic requirements, including the required heat duty, acceptable pressure drops on both sides, and practical geometric constraints. The exchanger must therefore provide sufficient heat-transfer area and an appropriate flow arrangement while remaining feasible from an engineering point of view.

Pasteurised orange juice is a valuable product because it combines **nutritional value, consumer safety, and commercial practicality**. Orange juice is widely consumed and is an important source of vitamins, especially vitamin C, as well as flavour compounds and sugars that make it an attractive food product. However, untreated juice is a perishable product and can contain microorganisms that shorten shelf life and create safety risks. Pasteurisation reduces microbial activity, allowing the juice to be stored, transported, and sold more reliably on an industrial scale. For this reason, pasteurised orange juice has both clear consumer value and strong economic importance in food processing.

A shell-and-tube heat exchanger is a reasonable choice for this duty because it is a **robust and conservative design** for heating a food liquid that may foul and that requires reliable operation. In this case, orange juice is more difficult to handle than a simple clean liquid because it can leave deposits on heat-transfer surfaces, making cleanability an important design issue. A shell-and-tube exchanger is well suited to such service because the tube side can be assigned to the juice, making cleaning and maintenance more manageable. In addition, shell-and-tube exchangers can operate safely under pressurised conditions, allow flexible combinations of tube passes and shell-side baffling, and are widely used in industry. Although more compact exchanger types such as plate heat exchangers may offer higher heat-transfer coefficients, the shell-and-tube design is more tolerant of fouling and mechanically more robust [2].

Another possible exchanger type is the plate heat exchanger, which provides more heat-transfer area for the same volume. However, the shell-and-tube heat exchanger is more conservative and more suitable for this particular duty because of its better fouling tolerance and greater mechanical robustness, as summarised in table 2.

Comparison of exchanger types

Table 2: Comparison of candidate exchanger types for this duty

Type	Shell-and-tube	Plate heat exchanger
Fouling tolerance	Better tolerance to fouling and suspended material; performance is less sensitive to partial blockage	More sensitive to fouling because of narrow flow channels and tighter passages
Cleanability	Tube side can be cleaned more directly; mechanically robust for cleaning-intensive service	Can be easy to dismantle and clean, but narrow passages are less forgiving for viscous or fouling food streams
Pressure capability	Generally more suitable for higher-pressure operation and pressure-drop flexibility	Usually less favourable for higher-pressure duties than shell-and-tube designs
Thermal performance	Lower heat-transfer efficiency per unit area, so a larger heat-transfer area is often required	Higher heat-transfer coefficients and more compact heat-transfer surface for the same duty
Mechanical robustness	Stronger and more tolerant of demanding operating conditions and conservative industrial service	More compact but mechanically less robust for severe conditions
Suitability for juice pasteurisation	More suitable because it is more tolerant to fouling, easier to justify for a viscous food liquid, and more conservative for hygienic heating duty	Attractive because of compactness and high thermal efficiency, but less suitable because fouling and cleaning are more critical for orange juice service

2 Design Decisions and Discussion

2.1 Initial Design Basis

Several literature sources were used to define the orange-juice properties adopted in the design basis. For clarified orange juice at approximately 12 Brix, published rheological and thermophysical data were reviewed over the temperature range relevant to the present duty. On that basis, the juice was modelled using representative bulk properties, with viscosity treated as an **apparent viscosity** for the operating temperature range considered. This provides a consistent basis for the Reynolds-, Prandtl-, and pressure-drop calculations while remaining aligned with the available literature on clarified orange-juice flow behaviour and thermophysical properties [3, 4, 5, 6, 7, 8].

Table 3: Orange juice properties adopted for the design basis

Property	Symbol	Adopted value	Source
Density	ρ_{juice}	$1052\,\text{kg/m}^3$	[7, 5]
Specific heat capacity	$C_{p,\text{juice}}$	$3900\,\text{J/(kg K)}$	[5, 6]
Thermal conductivity	k_{juice}	$0.50\,\text{W/(m K)}$	[5, 8]
Apparent viscosity at inlet (25 °C)	$\mu_{\text{juice,in}}$	$6.0 \cdot 10^{-4}\,\text{Pa s}$	[4, 3]
Apparent viscosity at outlet (98 °C)	$\mu_{\text{juice,out}}$	$5.0 \cdot 10^{-4}\,\text{Pa s}$	[4, 3]
Fouling resistance	$R_{f,\text{juice}}$	$3.0 \cdot 10^{-4}\,\text{m}^2\text{K/W}$	[1]

Table 4: Hot-water properties adopted for the design basis

Property	Symbol	Adopted value	Source
Density	ρ_{water}	$945\,\text{kg/m}^3$	[9]
Specific heat capacity	$C_{p,\text{water}}$	$4180\,\text{J/(kg K)}$	[9]
Thermal conductivity	k_{water}	$0.68\,\text{W/(m K)}$	[9]
Dynamic viscosity	μ_{water}	$2.31 \cdot 10^{-4}\,\text{Pa s}$	[9]
Fouling resistance	$R_{f,\text{water}}$	$1.8 \cdot 10^{-4}\,\text{m}^2\text{K/W}$	[2]

The values in table 3 were adopted as **design values** for clarified orange juice at approximately 12 Brix over the operating range relevant to this duty. Density and specific heat capacity were taken as representative values from the cited thermophysical-property data, while the viscosity values were treated as **apparent viscosities** at the inlet and outlet conditions in order to keep the hydraulic and heat-transfer calculations internally consistent [3, 4, 5, 6, 7]. The thermal conductivity was taken as a representative literature value and then held constant throughout the calculations. These quantities were therefore used as consolidated engineering design values derived from the cited property sources rather than from a single temperature-specific dataset.

As stated in the design brief, the minimum allowable hot-water outlet temperature is 108 °C [1]. To provide a small design margin above this requirement, the hot-water outlet temperature was fixed at 110 °C. All other design constraints were retained as specified in the project brief.

Table 5: Design basis

Parameter	Symbol	Value
Orange juice mass flow rate	$\dot{m}_{\text{juice}}$	4.676 kg/s
Orange juice inlet temperature	$T_{\text{juice,in}}$	25 °C
Orange juice outlet temperature	$T_{\text{juice,out}}$	98 °C
Hot water inlet temperature	$T_{\text{water,in}}$	130 °C
Hot water outlet temperature	$T_{\text{water,out}}$	110 °C
Tube-side pressure-drop limit	$\Delta P_{\text{tube,max}}$	0.5 bar
Shell-side pressure-drop limit	$\Delta P_{\text{shell,max}}$	0.5 bar

2.2 Major Design Decisions

2.2.1 Fluid Allocation

According to Sinnott, fouling removal is simpler on the tube side than on the shell side [2]. Since orange juice is the more fouling-prone stream and also the food product, it was placed in the tubes, while hot water was assigned to the shell side.

2.2.2 Exchanger Configuration

A conventional **TEMA BEM** shell-and-tube exchanger was selected [10, 2]. In TEMA notation, **B** denotes a bonnet front head, **E** a single-pass shell, and **M** a fixed tubesheet rear end. This configuration was adopted because it is simple, compact, and appropriate for a standard pasteurisation duty.

2.2.3 Tube Layout and Passes

A **square tube layout** was selected. Although triangular layouts are often thermally favourable, square layouts are easier to clean and more suitable where fouling and hygiene are important considerations. Sinnott recommends a tube pitch of about $1.25d_o$, which was adopted here [2].

Standard 6 m tubes were used, with $d_o = 25.0$ mm and $d_i = 21.8$ mm. The final selection was therefore **66 tubes in 6 passes** (11 tubes per pass), which gave an available area of 31.10 m^2, a required area of 29.33 m^2, and an area surplus of 6.0 %. The resulting pitch ratio was

$$\frac{p_t}{d_o} = \frac{31.25}{25.0} = 1.25$$

which matches the usual Sinnott recommendation for shell-and-tube exchangers [2].

2.2.4 Baffle Design

The exchanger uses **single-segmental vertical-cut baffles**, the most common arrangement for shell-and-tube service [2]. This configuration was chosen because it promotes shell-side crossflow and mixing while remaining mechanically straightforward.

For the final design, the shell diameter was 440 mm and the baffle spacing was 220 mm, so

$$\frac{B}{D_s} = \frac{220}{440} = 0.50$$

Sinnott recommends a central baffle spacing of about $0.3D_s$ to $0.5D_s$, so the final value lies at the upper limit of the recommended range [2].

The baffle cut was fixed at **20%**. Sinnott quotes a usual design range of about 20–25% for single-segmental baffles, so the selected value is also within the recommended range [2]. The cut was taken to be vertical rather than horizontal. This does not alter the main crossflow mechanism, but it is helpful in reducing stagnant regions at the bottom of the shell.

The final geometry gives an effective number of central crossflow rows of $N_{\text{cross}} = 8.45$, which is considerably more conventional for Bell-method evaluation than the earlier open-shell trial geometries. Because the selected central baffle spacing does not divide the tube length exactly, the remaining length was split equally between the two end zones, giving front and back spacings of 30 mm each and 27 central baffle spacings of 220 mm.

When the shell-side design was refined from the Kern method to **Bell's method**, the inclusion of leakage, bypass, and window effects reduced the predicted shell-side thermal performance. Even after these corrections, however, the final exchanger retained both a positive area margin and an acceptable shell-side pressure drop *without* sealing strips. This was achieved because the final geometry already lay close to the recommended design ranges for tube pitch ratio, baffle spacing ratio, and baffle cut, so excessive shell-side opening was no longer necessary.

2.2.5 Materials of Construction

AISI 316L stainless steel was selected for all wetted parts because of its corrosion resistance, hygienic suitability, and widespread use in food-processing equipment. In the present design, this includes the tubes, baffles, tubesheets, shell-side internals, support rods, spacers, and any sealing-strip material if later required. External non-wetted components could, in practice, be manufactured from a less expensive structural material, but material optimisation outside the wetted envelope was not pursued further here.

2.3 Design Development Path

The initial full design was developed using the simplified procedure presented by Sinnott, i.e. the Kern method. This first version used 4 tube passes and 25.0 mm OD tubes. Although the thermal area margin was acceptable, the main weakness of the design was the shell-side pressure drop. The large baffle cut of 40% helped hydraulically, but the exchanger geometry was still not satisfactory overall.

The second iteration attempted to address this issue indirectly by increasing the shell diameter through an increase in the number of tubes. In practice, however, this did not resolve the problem. It was therefore decided to move to a higher number of tube passes.

In the third iteration, the tube count was kept at 84, but the exchanger was redesigned with 6 passes. This increased the tube-side pressure drop, although the tube-side limit was never the controlling constraint. At the same time, the shell-side problem from the earlier design was resolved. However, the exchanger then had an excessively large thermal surplus, with an area margin of 42.3%. Such an overdesigned surface was undesirable because it implied unnecessary excess area and reduced the overall balance of the design.

Reducing the tube count from 84 to 72 approximately halved the surplus area, but the baffle cut still remained too large for a balanced final configuration. The next iteration therefore focused on reducing the baffle cut.

The fifth and sixth iterations were devoted to balancing the baffle cut and baffle spacing so that the design would fall within the usual industrial range of about $0.3D_s$ to $0.5D_s$. Varying the baffle spacing between 150 mm and 250 mm, and the baffle cut between 40% and 20%, showed that the most suitable compromise was obtained at 220 mm spacing and 20% cut.

In the seventh iteration, the final design was checked against all project requirements. The remaining area margin was sufficient to accommodate practical allowances associated with baffles, supports, and local contact regions. In addition, no sealing strips were required in the final configuration. Their role would be to increase the shell-side heat-transfer coefficient, but at the expense of a higher pressure drop. Since the present design already retained a positive area margin, one sealing-strip pair could still be introduced later, if needed, without creating a serious risk of overheating or excessive pressure drop.

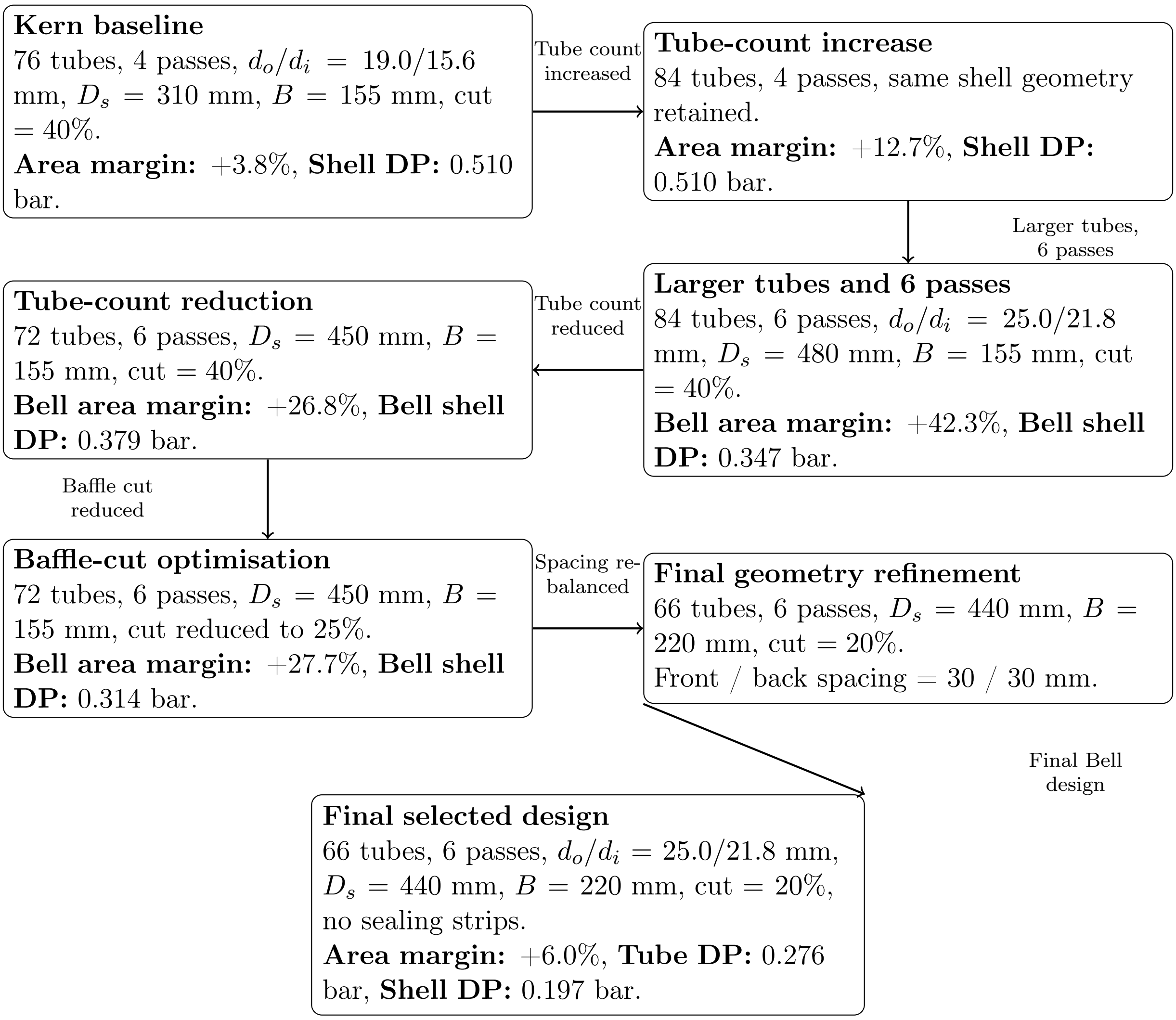

Figure 1: Design iteration pathway from the early Kern-based sizing to the final Bell's-method shell-side design.

2.4 Design summary

Table 6 combines the main exchanger geometry, the Bell's-method shell-side geometric quantities, and several constructional selections used for layout definition and shell-side blockage estimation.

Table 6: Final design dimensions

Item	Value	Unit / note
Tube outer / inner diameter	25.0 / 21.8	mm
Tube length / tube passes	6.0 / 6	m / –
Number of tubes / tubes per pass	66 / 11	–
Tube layout / tube pitch / pitch ratio	Square / 31.25 / 1.25	mm / –
Partition lane width / axis shift	25.0 / 0.50	mm / pitch
Bundle diameter / shell ID (calc.) / shell ID (selected)	423.2 / 435.4 / 440.0	mm
Bundle-to-shell clearance	12.2	mm
Tube-to-baffle clearance / shell-to-baffle clearance	0.80 / 1.60	mm
Baffle type / orientation	Single-segmental / vertical cut	–
Baffle cut / central spacing	20 / 220	% / mm
Inlet spacing / outlet spacing / total baffles	30 / 30 / 27	mm / –
Baffle thickness / spacer length	4.0 / 216.0	mm
Tie-rod diameter / number of tie rods	12.0 / 4	mm / –
Spacer count from layout	52	–
Cross-flow area / raw cross-flow area	0.01936 / 0.01936	m^2
Rod blockage / window area / effective window area	0.00000 / 0.02165 / 0.01704	m^2
Leakage area A_{sb} / leakage area A_{tb}	0.00177 / 0.00332	m^2
Bypass area A_{bp}	0.00538	m^2
Tube-side nozzle ID / shell-side nozzle ID	65.0 / 125.0	mm
Tube-side nozzle / shell-side nozzle	DN65 / DN125	–
Juice nozzle velocity / water nozzle velocity	1.339 / 1.373	m/s
Tube length blocked by baffles	108.0	mm
Wetted-part material / strip material	AISI 316L / AISI 316L	stainless steel

3 Safety, Health and Environment (SHE)

The main SHE concerns in this design arise from bringing together a hot pressurised utility stream and a food-product stream within the same exchanger. Pressurised hot water is used on the shell side, while orange juice flows through the tubes, so the design must address thermal hazards, pressure containment, and the risk of contaminating the product. Hygienic operation is also important, since orange juice can foul heat-transfer surfaces and make cleaning more difficult. The detailed effects of rapid heating on juice quality and the detailed fouling chemistry are not considered in this report.

Local hydrodynamic effects must also be considered. High local velocities in restricted shell-side regions can promote erosion, impingement, or flow-induced vibration if the internal geometry is poorly proportioned. In the present design, the shell-side bulk velocity was $0.870\,\mathrm{m\,s^{-1}}$, and the final geometry was selected so that both shell-side and tube-side pressure drops remained below the specified limits. The use of closely spaced baffles and standard support hardware provides regular tube support along the bundle length, which reduces the likelihood of excessive tube movement under the selected operating conditions. A dedicated vibration calculation was not included in this report, but the final configuration was chosen to remain within a conservative hydraulic regime rather than relying on unusually high local velocities or excessively open shell-side geometry.

3.1 General SHE Considerations

- **Thermal hazards:** The shell side contains hot pressurised water at up to 130 °C, which creates a clear burn hazard during operation and maintenance. Insulation is therefore required, and exposed hot surfaces should be clearly marked.
- **Pressure hazards:** Both sides of the exchanger operate under pressure, so any loss of containment could release hot liquid and endanger personnel. For this reason, the exchanger must remain within the specified pressure-drop limits and use a mechanically resistant configuration.
- **Food-product contamination risk:** Because orange juice is a food product, contamination from utility fluid, corrosion products, or deposits must be avoided as far as possible. The choice of stainless steel wetted parts and a conservative shell-and-tube arrangement helps reduce this risk.
- **Cleaning / maintenance considerations:** Orange juice can foul heat-transfer surfaces, so ease of cleaning is both an SHE issue and an operational requirement. Placing the juice on the tube side makes cleaning more manageable and supports hygienic procedures such as CIP.
- **Material compatibility / hygiene:** AISI 316L stainless steel was chosen for wetted parts because of its corrosion resistance and its suitability for hygienic food-service applications. This helps limit material degradation and supports sanitary operation over time.

3.2 Consequence of Tube Failure

If a tube fails, hot water from the shell side may come into contact with orange juice on the tube side, since flow would tend to occur from the higher-pressure side to the lower-pressure side. The most serious consequence would be contamination of the food product, making it unsuitable for use. A reasonable mitigation would be to provide detection on the juice outlet line, for example by temperature or conductivity anomaly monitoring, together with isolation valves and a diversion arrangement to prevent further contamination of the product stream.

4 Thermal Calculations

For the hot-water side, the thermophysical properties were treated as **representative bulk design values** at a mean shell-side temperature of approximately 120 °C. Accordingly, $C_{p,\text{water}} = 4180\,\text{J}\,\text{kg}^{-1}\,\text{K}^{-1}$ was used in the energy balance, while $\rho_{\text{water}} = 945\,\text{kg}\,\text{m}^{-3}$, $k_{\text{water}} = 0.68\,\text{W}\,\text{m}^{-1}\,\text{K}^{-1}$, and $\mu_{\text{water}} = 2.31 \cdot 10^{-4}\,\text{Pa}\,\text{s}$ were adopted as representative liquid-water properties from *Perry's Chemical Engineers' Handbook* [9].

4.1 Heating Water Flow Rate

The required hot-water flow rate was obtained from the energy balance:

$$Q = \dot{m}_{\text{juice}} C_{p,\text{juice}} (T_{\text{juice,out}} - T_{\text{juice,in}}) = 4.676 \times 3900 \times (98 - 25) = 1.331 \cdot 10^6\,\text{W} \tag{1}$$

$$\dot{m}_{\text{water}} = \frac{Q}{C_{p,\text{water}}(T_{\text{water,in}} - T_{\text{water,out}})} = \frac{1.331 \times 10^6}{4180 \times (130 - 110)} = 15.924\,\text{kg/s} \tag{2}$$

4.2 Corrected Log Mean Temperature Difference

For the final design,

$$\Delta T_1 = 130 - 98 = 32\,\text{K}, \qquad \Delta T_2 = 110 - 25 = 85\,\text{K} \tag{3}$$

$$\Delta T_{\text{lm}} = \frac{\Delta T_2 - \Delta T_1}{\ln(\Delta T_2/\Delta T_1)} = \frac{85 - 32}{\ln(85/32)} = 54.26\,\text{K} \tag{4}$$

For the correction chart,

$$R = \frac{T_{\text{hot,in}} - T_{\text{hot,out}}}{T_{\text{cold,out}} - T_{\text{cold,in}}} = \frac{130 - 110}{98 - 25} = 0.274 \tag{5}$$

$$S = \frac{T_{\text{cold,out}} - T_{\text{cold,in}}}{T_{\text{hot,in}} - T_{\text{cold,in}}} = \frac{98 - 25}{130 - 25} = 0.695 \tag{6}$$

From Sinnott Fig. 12.19,

$$F = 0.9 \tag{7}$$

for a one-shell-pass multipass exchanger. Therefore,

$$\Delta T_{\text{corr}} = F \Delta T_{\text{lm}} = 0.9 \times 54.26 = 48.83\,\text{K} \tag{8}$$

4.3 Sizing of Tubes and Shell

The final design uses 66 straight tubes in 6 passes, with $d_o = 25.0\,\text{mm}$, $d_i = 21.8\,\text{mm}$, $L_t = 6.0\,\text{m}$, and square pitch $p_t = 31.25\,\text{mm}$. From Sinnott Table 12.4 for square layout with $p_t/d_o = 1.25$ and 6 tube passes, $K_1 = 0.0402$ and $n_1 = 2.617$, giving a bundle diameter of 423.2 mm. From Sinnott Fig. 12.10, the shell–bundle clearance was taken as 12.2 mm, giving a calculated shell ID of 435.4 mm, rounded to a selected shell ID of 440.0 mm.

Table 7: Final geometric selection

Quantity	Symbol	Value
Tube OD	d_o	25.0 mm
Tube ID	d_i	21.8 mm
Tube length	L_t	6.0 m
Number of tubes / passes	N_t/N_p	66 / 6
Tube pitch	p_t	31.25 mm
Bundle diameter	D_b	423.2 mm
Shell ID (selected)	D_s	440.0 mm

4.4 Inside (Tube-side) Heat Transfer Coefficient

The tube-side flow area and velocity were

$$A_{\text{flow,tube}} = \frac{N_t}{N_p}\frac{\pi d_i^2}{4} = 11 \times \frac{\pi(0.0218)^2}{4} = 4.11 \cdot 10^{-3}\,\text{m}^2 \tag{9}$$

$$v_{\text{juice}} = \frac{\dot{m}_{\text{juice}}}{\rho_{\text{juice}} A_{\text{flow,tube}}} = \frac{4.676}{1052 \times 4.11 \times 10^{-3}} = 1.083\,\text{m}\,\text{s}^{-1} \tag{10}$$

Using $\mu_{\text{juice}} = 5.0 \cdot 10^{-4}\,\text{Pa}\,\text{s}$,

$$\text{Re}_{\text{juice}} = 49655, \qquad \text{Pr}_{\text{juice}} = 3.90 \tag{11}$$

The Dittus–Boelter correlation is applicable because

$$\text{Re}_{\text{juice}} = 49655 > 10^4, \qquad 0.7 < \text{Pr}_{\text{juice}} = 3.90 < 160, \qquad \frac{L_t}{d_i} = \frac{6.0}{0.0218} \approx 275 > 60 \tag{12}$$

Hence,

$$\text{Nu}_{\text{juice}} = 0.023\,\text{Re}_{\text{juice}}^{0.8}\text{Pr}_{\text{juice}}^{0.4} = 226.43 \tag{13}$$

$$h_i = \frac{\text{Nu}_{\text{juice}} k_{\text{juice}}}{d_i} = \frac{226.43 \times 0.50}{0.0218} = 5193.3\,\text{W}\,\text{m}^{-2}\,\text{K}^{-1} \tag{14}$$

The wall-viscosity correction was neglected:

$$\left(\frac{\mu}{\mu_w}\right)^{0.14} = 1 \tag{15}$$

4.5 Outside (Shell-side) Heat Transfer Coefficient

The shell-side coefficient was evaluated by **Bell's method** following Sinnott [2]. For the final design,

$$A_{\text{cross,shell}} = 0.019\,36\,\text{m}^2, \qquad v_{\text{water}} = 0.870\,\text{m}\,\text{s}^{-1}, \qquad \text{Re}_{\text{water}} = 88078 \tag{16}$$

and

$$h_o = h_{oc} F_n F_w F_b F_L \tag{17}$$

The main Bell-method geometric quantities were

$$A_L = A_{sb} + A_{tb} = 0.00177 + 0.00332 = 0.005\,09\,\text{m}^2, \qquad \frac{A_L}{A_s} = \frac{0.00509}{0.01936} = 0.263 \tag{18}$$

$$A_b = A_{bp} = 0.005\,38\,\mathrm{m}^2, \qquad \frac{A_b}{A_s} = \frac{0.00538}{0.01936} = 0.278 \tag{19}$$

For the window region,

$$A_{w,\text{gross}} = 0.021\,65\,\mathrm{m}^2, \qquad A_w = 0.017\,04\,\mathrm{m}^2, \qquad R_w = 0.285 \tag{20}$$

and

$$N_{wv} = 2.816, \qquad N_{\text{cross}} = N_{cv} = 8.448 \tag{21}$$

From Sinnott Fig. 12.31 for Re = 88078 and square layout with $p_t/d_o = 1.25$,

$$j_h = 3.5 \times 10^{-3} \tag{22}$$

Thus,

$$\frac{h_{oc} d_o}{k_f} = j_h \mathrm{Re}\mathrm{Pr}^{1/3} \left(\frac{\mu}{\mu_w}\right)^{0.14} \tag{23}$$

with $(\mu/\mu_w)^{0.14} = 1$, giving

$$h_{oc} = \frac{k_f}{d_o} j_h \mathrm{Re}\mathrm{Pr}^{1/3} = \frac{0.68}{0.0250} \times 3.5 \times 10^{-3} \times 88078 \times 1.42^{1/3} = 9424.6\,\mathrm{W\,m^{-2}\,K^{-1}} \tag{24}$$

From the Bell-method charts,

$$F_n = 0.98 \tag{25}$$

at $N_{\text{cross}} = 8.448$, and from Sinnott Fig. 12.33, using $R_w = 0.285$,

$$F_w = 1.09 \tag{26}$$

The bypass correction was evaluated from the Bell–Sinnott bypass equation. For Re > 100, $\alpha = 1.35$, and with no sealing strips assumed, $N_s = 0$, so

$$F_b = \exp\left[-\alpha \frac{A_b}{A_s}\left(1 - \left(\frac{2N_s}{N_{cv}}\right)^{1/3}\right)\right] = \exp\left[-1.35 \times 0.278\right] = 0.687 \tag{27}$$

For leakage, using $\beta_L = 0.267$ from Sinnott Fig. 12.35,

$$F_L = 1 - \beta_L \left(\frac{A_{tb} + 2A_{sb}}{A_L}\right) \tag{28}$$

which gives

$$F_L = 1 - 0.267\left(\frac{0.00332 + 2 \times 0.00177}{0.00509}\right) = 0.640 \tag{29}$$

Therefore,

$$F_n = 0.98, \qquad F_w = 1.09, \qquad F_b = 0.687, \qquad F_L = 0.640 \tag{30}$$

and

$$h_o = h_{oc} F_n F_w F_b F_L = 9424.6 \times 0.98 \times 1.09 \times 0.687 \times 0.640 = 4427.8\,\mathrm{W\,m^{-2}\,K^{-1}} \tag{31}$$

4.6 Fouling and Tube-Wall Resistances

The fouling resistances were treated as **fouling allowances** for a food-product tube side and a hot-water utility side. In the present work,

$$R_{f,\text{juice}} = 3.0 \cdot 10^{-4}\,\text{m}^2\,\text{K}\,\text{W}^{-1}, \qquad R_{f,\text{water}} = 1.8 \cdot 10^{-4}\,\text{m}^2\,\text{K}\,\text{W}^{-1} \tag{32}$$

were adopted as conservative design values [2].

For AISI 316L stainless steel, the tube-wall thermal conductivity was taken as

$$k_w = 16.3\,\text{W}\,\text{m}^{-1}\,\text{K}^{-1} \tag{33}$$

using a representative handbook value from *Perry's Chemical Engineers' Handbook* [9]. Therefore,

$$R_w = \frac{d_o \ln(d_o/d_i)}{2k_w} = \frac{0.0250 \ln(0.0250/0.0218)}{2 \times 16.3} = 1.05 \cdot 10^{-4}\,\text{m}^2\,\text{K}\,\text{W}^{-1} \tag{34}$$

4.7 Overall Heat Transfer Coefficient

The total resistance based on the outer tube area was

$$R_{\text{tot}} = \frac{1}{h_o} + R_{f,\text{water}} + R_w + \frac{d_o}{d_i}\left(\frac{1}{h_i} + R_{f,\text{juice}}\right) = 1.076 \cdot 10^{-3}\,\text{m}^2\,\text{K}\,\text{W}^{-1} \tag{35}$$

therefore

$$U = \frac{1}{R_{\text{tot}}} = \frac{1}{1.076 \times 10^{-3}} = 929.6\,\text{W}\,\text{m}^{-2}\,\text{K}^{-1} \tag{36}$$

4.8 Thermal Performance Summary

Table 8: Thermal calculation summary

Quantity	Symbol	Value
Heat duty	Q	$1.331 \cdot 10^6$ W
Water flow rate	$\dot{m}_{\text{water}}$	15.924 kg/s
Corrected LMTD	ΔT_{corr}	48.83 K
Tube-side HTC	h_i	$5193.3\,\text{W}\,\text{m}^{-2}\,\text{K}^{-1}$
Shell-side HTC	h_o	$4427.8\,\text{W}\,\text{m}^{-2}\,\text{K}^{-1}$
Overall HTC	U	$929.6\,\text{W}\,\text{m}^{-2}\,\text{K}^{-1}$
Required area	A_{req}	$29.33\,\text{m}^2$
Available area	A_{avail}	$31.10\,\text{m}^2$
Area margin	—	6.0 %

5 Hydraulic Calculations

5.1 Sizing of Nozzles

For the final design,

$$\dot{V}_{\text{juice}} = 4.45 \cdot 10^{-3}\,\text{m}^3\,\text{s}^{-1}, \qquad A_{\text{noz,juice}} = \frac{\pi (0.065)^2}{4} = 3.32 \cdot 10^{-3}\,\text{m}^2, \qquad v_{\text{noz,juice}} = \frac{\dot{V}_{\text{juice}}}{A_{\text{noz,juice}}} = 1.339\,\text{m}\,\text{s}^{-1} \tag{37}$$

$$\dot{V}_{\text{water}} = \frac{\dot{m}_{\text{water}}}{\rho_{\text{water}}} = \frac{15.924}{945} = 1.685 \cdot 10^{-2}\,\text{m}^3\,\text{s}^{-1} \tag{38}$$

$$A_{\text{noz,water}} = \frac{\pi(0.125)^2}{4} = 1.227 \cdot 10^{-2}\,\text{m}^2, \qquad v_{\text{noz,water}} = \frac{\dot{V}_{\text{water}}}{A_{\text{noz,water}}} = 1.373\,\text{m}\,\text{s}^{-1} \tag{39}$$

Thus, the selected nozzles were DN65 on the tube side and DN125 on the shell side.

5.2 Tube-side Pressure Drop

Using $\text{Re}_{\text{juice}} = 49655$, the Blasius correlation gives

$$f_D = \frac{0.3164}{\text{Re}^{0.25}} = 0.0212 \tag{40}$$

with

$$L_{\text{tot}} = N_p L_t = 36.0\text{ m}, \qquad \frac{\rho_{\text{juice}} v_{\text{juice}}^2}{2} = \frac{1052 \times 1.083^2}{2} = 616.5\,\text{Pa} \tag{41}$$

Hence,

$$\Delta P_{\text{fric}} = f_D \frac{L_{\text{tot}}}{d_i}\left(\frac{\rho_{\text{juice}} v_{\text{juice}}^2}{2}\right) = 0.216\,\text{bar} \tag{42}$$

$$\Delta P_{\text{return}} = 1.5 \times 5 \times 616.5 = 0.046\,\text{bar} \tag{43}$$

$$\Delta P_{\text{noz}} = 1.5 \times \frac{1052 \times 1.339^2}{2} = 0.014\,\text{bar} \tag{44}$$

Therefore,

$$\Delta P_{\text{tube,tot}} = \Delta P_{\text{fric}} + \Delta P_{\text{return}} + \Delta P_{\text{noz}} = 0.216 + 0.046 + 0.014 = 0.276\,\text{bar} < 0.5\,\text{bar} \tag{45}$$

5.3 Shell-side Pressure Drop

Bell's method was used following Sinnott [2]. For the final design,

$$\text{Re}_{\text{water}} = 88078, \qquad j_f = 4.0 \times 10^{-2} \tag{46}$$

and

$$\frac{\rho_{\text{water}} v_{\text{water}}^2}{2} = \frac{945 \times 0.870^2}{2} = 357.6\,\text{Pa} \tag{47}$$

Using $N_{\text{cross}} = 8.448$,

$$\Delta P_i = 8 j_f N_{\text{cross}} \left(\frac{\rho_{\text{water}} v_{\text{water}}^2}{2}\right) = 8 \times 0.040 \times 8.448 \times 357.6 \approx 0.010\,\text{bar} \tag{48}$$

The corrected crossflow term was

$$\Delta P_c = \Delta P_i F_b' F_L' \tag{49}$$

with

$$F_b' = \exp(-4.0 \times 0.278) = 0.329 \tag{50}$$

and

$$F_L' = 1 - 0.482\left(\frac{0.00332 + 2 \times 0.00177}{0.00509}\right) = 0.350 \tag{51}$$

Hence,

$$\Delta P_c = 0.010 \times 0.329 \times 0.350 \approx 0.001\,\text{bar} \tag{52}$$

The window-zone term was

$$\Delta P_w = F'_L \left(2 + 0.6 N_{wv}\right) \frac{\rho_{\text{water}} u_z^2}{2} \tag{53}$$

with

$$u_w = \frac{15.924}{945 \times 0.01704} = 0.989\,\mathrm{m\,s^{-1}}, \qquad u_z = \sqrt{0.989 \times 0.870} = 0.928\,\mathrm{m\,s^{-1}} \tag{54}$$

and $N_{wv} = 2.816$, giving

$$\Delta P_w = 0.005\,\mathrm{bar} \tag{55}$$

The end-zone term was

$$\Delta P_e = \Delta P_i \left(\frac{N_{wv} + N_{\text{cross}}}{N_{\text{cross}}}\right) F'_b \approx 0.004\,\mathrm{bar} \tag{56}$$

Using $N_b = 27$,

$$\Delta P_{\text{shell,fric}} = 2\Delta P_e + \Delta P_c (N_b - 1) + N_b \Delta P_w = 0.179\,\mathrm{bar} \tag{57}$$

For the shell-side nozzles, Sinnott recommends 1.5 velocity heads at the inlet and 0.5 at the outlet. Thus,

$$\Delta P_{\text{noz,shell,in}} = 1.5 \left(\frac{\rho_{\text{water}} v_{\text{noz,water}}^2}{2}\right) \approx 0.014\,\mathrm{bar} \tag{58}$$

$$\Delta P_{\text{noz,shell,out}} = 0.5 \left(\frac{\rho_{\text{water}} v_{\text{noz,water}}^2}{2}\right) \approx 0.004\,\mathrm{bar} \tag{59}$$

Hence,

$$\Delta P_{\text{noz,shell}} = 0.014 + 0.004 = 0.018\,\mathrm{bar} \tag{60}$$

and

$$\Delta P_{\text{shell,tot}} = \Delta P_{\text{shell,fric}} + \Delta P_{\text{noz,shell}} = 0.179 + 0.018 = 0.197\,\mathrm{bar} \tag{61}$$

5.4 Hydraulic Performance Summary

Table 9: Hydraulic calculation summary

Quantity	Symbol	Value
Tube-side velocity	v_{juice}	$1.083\,\mathrm{m\,s^{-1}}$
Tube-side pressure drop	$\Delta P_{\text{tube,tot}}$	0.276 bar
Shell-side velocity	v_{water}	$0.870\,\mathrm{m\,s^{-1}}$
Shell-side pressure drop	$\Delta P_{\text{shell,tot}}$	0.197 bar
Juice nozzle diameter	$d_{\text{noz,juice}}$	65 mm
Water nozzle diameter	$d_{\text{noz,water}}$	125 mm

6 Completed Data Sheet

Heat Exchanger Data Sheet

Client: University of Cambridge	Area: CEBT IB	Item no.: HX-01

Heating medium: Hot water		
No of units: 1	Type: TEMA BEM	Orientation: Horizontal

	Units	**Shell Fluid**		**Tube Fluid**	
		In	**Out**	**In**	**Out**
Total fluid flow	**kg s^{-1}**	15.923	15.923	4.676	4.676
Liquid	**kg s^{-1}**	15.923	15.923	4.676	4.676
Vapour	**kg s^{-1}**	0	0	0	0
Non condensable	**kg s^{-1}**	0	0	0	0
Steam	**kg s^{-1}**	0	0	0	0
Water	**kg s^{-1}**	15.923	15.923	0	0
Temperature	**°C**	130	110	25	98
Mol. Wt of vapour + NC		N/A	N/A	N/A	N/A
Liquid density	**kg m^{-3}**	945	945	1052	1052
Liquid viscosity	**Pa s**	0.0002	0.0002	0.0006	0.0005
Vapour + NC viscosity	**Pa s**	N/A	N/A	N/A	N/A
Liquid sp. heat	**kJ kg^{-1} K^{-1}**	4.18	4.18	3.90	3.90
Vapour + NC sp. heat	**kJ kg^{-1} K^{-1}**	N/A	N/A	N/A	N/A
Liquid thermal conductivity	**W m^{-1} K^{-1}**	0.68	0.68	0.50	0.50
Vap. + NC thermal conduct.	**W m^{-1} K^{-1}**	N/A	N/A	N/A	N/A
Latent heat	**kJ kg^{-1}**	N/A	N/A	N/A	N/A
Surface tension	**N m^{-1}**	N/A	N/A	N/A	N/A
Dew pt/bubble pt	**°C**	N/A	N/A	N/A	N/A
Freeze pt/pour pt	**°C**	N/A	N/A	N/A	N/A
Inlet pressure	**bar**	6.0		4.0	
Allowable press. drop	**bar**	0.5		0.5	
Fouling resistance	**m^2 K W^{-1}**	0.00018		0.00030	
Heat exchanged	**MW**	1.33			
Min./max. operating temp	**°C**	130	110	25	98
Max. operating pressure	**bar**	6.0		4.0	
Min. design pressure	**bar**	N/A		N/A	
Relief valve set pressure	**bar**	7.0		5.0	
Design pressure	**bar**	7.0		5.0	
Cyclic service		No		No	
Materials		AISI 316L		AISI 316L	
Corrosion allowance	**mm**	0		0	
Line size	**mm**	125	125	65	65
Heat treatment		None		None	
Hazards		Hot water		Food Product	
Insulation		Insulate		No	
Cleaning		Std cleaning		CIP	
Over design multiplier		**N/A**		**N/A**	

Rev no	0			
Eng/date	11 Mar 2026			
Checked/date	—			
Approved/date	—			

7 Nomenclature

Symbol	Units	Meaning
A	m^2	Area
A_b	m^2	Bundle-bypass flow area
A_L	m^2	Leakage flow area
A_s	m^2	Main shell-side crossflow area
A_w	m^2	Window flow area
C_p	$\mathrm{J\,kg^{-1}\,K^{-1}}$	Specific heat capacity at constant pressure
d	m	Diameter
D	m	Diameter
F	–	LMTD correction factor
F_n	–	Shell-side row/spacing correction factor
F_w	–	Shell-side window/cut correction factor
F_b	–	Shell-side bypass correction factor
F_L	–	Bell-method leakage correction factor for heat transfer
F'_L	–	Bell-method leakage correction factor for pressure drop
β_L	–	Bell-method leakage parameter for heat transfer
β'_L	–	Bell-method leakage parameter for pressure drop
f_D	–	Darcy friction factor
h	$\mathrm{W\,m^{-2}\,K^{-1}}$	Convective heat-transfer coefficient
h_{oc}	$\mathrm{W\,m^{-2}\,K^{-1}}$	Ideal shell-side heat-transfer coefficient
j_h	–	Bell-method shell-side heat-transfer factor
j_f	–	Bell-method shell-side friction factor
k	$\mathrm{W\,m^{-1}\,K^{-1}}$	Thermal conductivity
$\dot{m}$	$\mathrm{kg\,s^{-1}}$	Mass flow rate
N	–	Number
N_b	–	Number of baffles
N_c	–	Tubes in the central row
ΔP	bar	Pressure drop
Pr	–	Prandtl number
Q	W	Heat duty
r	–	Area ratio
R	–	LMTD correction chart parameter
S	–	LMTD correction chart parameter
R_f	$\mathrm{m^2\,K\,W^{-1}}$	Fouling resistance
R_w	$\mathrm{m^2\,K\,W^{-1}}$	Tube-wall thermal resistance
Re	–	Reynolds number
T	°C	Temperature
U	$\mathrm{W\,m^{-2}\,K^{-1}}$	Overall heat-transfer coefficient
v	$\mathrm{m\,s^{-1}}$	Fluid velocity
$\dot{V}$	$\mathrm{m^3\,s^{-1}}$	Volumetric flow rate
μ	Pa s	Dynamic viscosity
μ_w	Pa s	Fluid viscosity at wall temperature
ρ	$\mathrm{kg\,m^{-3}}$	Density

References

[1] University of Cambridge, Department of Chemical Engineering and Biotechnology. *CET IB Project 4: Part 1 — Design of a Shell and Tube Heat Exchanger*. Issue date: Friday 13 February 2026; course project brief. 2026.

[2] Ray Sinnott. *Chemical Engineering Design: Chemical Engineering Volume 6*. Used via extracted Chapter 12 PDF. Elsevier Science & Technology, 2005.

[3] Raquel Ibarz et al. "Flow behavior of clarified orange juice at low temperatures". In: *Journal of Texture Studies* 40.4 (2009), pp. 445–456. DOI: 10.1111/j.1745-4603.2009.00191.x.

[4] A. Ibarz, C. González, and S. Esplugas. "Rheology of clarified fruit juices. III: Orange juices". In: *Journal of Food Engineering* 21.4 (1994), pp. 485–494. DOI: 10.1016/0260-8774(94)90068-X.

[5] J. Telis-Romero et al. "Thermophysical properties of Brazilian orange juice as affected by temperature and water content". In: *Journal of Food Engineering* 38.1 (1998), pp. 27–40. DOI: 10.1016/S0260-8774(98)00107-1.

[6] Mauro Moresi and Marina Spinosi. "Engineering factors in the production of concentrated fruit juices. I. Fluid physical properties of orange juices". In: *Journal of Food Technology* 15.3 (1980), pp. 265–276. DOI: 10.1111/j.1365-2621.1980.tb00939.x.

[7] A. M. Ramos and A. Ibarz. "Density of juice and fruit puree as a function of soluble solids content and temperature". In: *Journal of Food Engineering* 35.1 (1998), pp. 57–63. DOI: 10.1016/S0260-8774(98)00004-1.

[8] Lemuel Diamante and Moyuru Umemoto. "Rheological Properties of Fruits and Vegetables: A Review". In: *International Journal of Food Properties* 18.6 (2015), pp. 1191–1210. DOI: 10.1080/10942912.2014.898653.

[9] Don W. Green and Marylee Z. Southard, eds. *Perry's Chemical Engineers' Handbook*. 9th ed. New York: McGraw-Hill Education, 2019.

[10] Tubular Exchanger Manufacturers Association. *Standards of the Tubular Exchanger Manufacturers Association*. 7th ed. TEMA, 1988.

[11] James F. Steffe. *Rheological Methods in Food Process Engineering*. 2nd ed. Freeman Press, 1992.

[12] Donald Q. Kern. *Process Heat Transfer*. New York: McGraw-Hill, 1950.

[13] Stefano Rozz et al. "Heat treatment of fluid foods in a shell and tube heat exchanger: Comparison between smooth and helically corrugated wall tubes". In: *Journal of Food Engineering* 79.1 (2007), pp. 249–254. DOI: 10.1016/j.jfoodeng.2006.01.050.

[14] J. Telis-Romero, V. R. N. Telis, and F. Yamashita. "Friction factors and rheological properties of orange juice". In: *Journal of Food Engineering* 40.1–2 (1999), pp. 101–106. DOI: 10.1016/S0260-8774(99)00045-X.

AI usage declaration

Gemini AI was used to revise the Python code and investigate bugs that appeared. NotebookLM was used for the preliminary search for papers on orange juice and generating the BibTeX file of references. ChatGPT was used to help improve the LaTeX presentation and make it beautiful and astonishing. Grammarly AI was used to improve grammar.